Journal of Molecular Medicine (2026) 104:69
https://doi.org/10.1007/s00109-026-02677-7

ORIGINAL ARTICLE

Pan-cancer ex vivo target evaluation of phosphodiesterase 3 A (PDE3A)

Kiesha Rice[1] · Noora Lehtinen[1,6] · Eetu Välimäki[1] · Janne Suhonen[1] · Pekka Taimen[2,3,4] · Kimmo Kettunen[2,3,4,8] · Sami Ventelä[2,5] · Juha Kononen[6] · Harri Sihto[7] · Juha K. Rantala[1,9]

Received: 4 December 2025 / Revised: 17 April 2026 / Accepted: 22 April 2026

Abstract

Phosphodiesterase 3 A (*PDE3A*) is a well-characterized enzyme that plays a crucial role in various cellular processes, including cAMP-mediated signaling, CREB-mediated induction of p21 and signaling through protein kinases A and G. PDE3A has also been suggested as an inflammation-associated stemness gene which upon interaction with protein *SLFN12*, leads to blocked protein translation and induction of apoptosis. PDE3A has been found to be highly expressed in several human cancer types including sarcomas, pancreatic ductal adenocarcinoma, non-small cell lung cancer and melanoma. *PDE3A* has thus emerged as a potential therapeutic cancer target. However, to fully understand the functional role and validate target potential of *PDE3A* in different human cancers, further research is needed. We report here a pan-cancer ex vivo study of *PDE3A* protein expression across 24 different cancer types represented by 59 different molecular subtypes correlated with ex vivo drug screening of *PDE3A-SLFN12* molecular glue anagrelide in 250 patient derived functional tumor models. Results of the study identify highest *PDE3A* expression in melanomas and across different histological subtypes of sarcomas. Correlating with the expression profile of *PDE3A*, anagrelide was found to display best therapeutic potential in sarcomas with high protein expression of both *PDE3A* and *SLFN12*, though sarcoma heterogeneity warrants further subtype-specific validation.

Key message

- 250 patient samples included in a functional ex vivo target validation study.
- Proteomic profiling identifies high expression of PDE3A in several cancer types.
- Anagrelide shows best therapeutic efficacy in sarcomas and melanomas.
- Expression of PDE3B expression not correlating with efficacy of anagrelide.

Keywords PDE3A · Pan-cancer · Target evaluation · RPPA · Ex vivo drug screening · Anagrelide

Kiesha Rice and Noora Lehtinen contributed equally to this work.

✉ Juha K. Rantala
rantala@misvik.com

1 Misvik Biology Oy, Karjakatu 35 B, Turku FI-20520, Finland

2 Institute of Biomedicine, University of Turku, Turku, Finland

3 FICAN West Cancer Center, University of Turku and Turku University Hospital, Turku, Finland

4 Department of Pathology, Laboratory Division, Turku University Hospital, Turku, Finland

5 Department for Otorhinolaryngology - Head and Neck Surgery, University of Turku and Turku University Hospital, Turku 20520, Finland

6 Docrates Cancer Center, Helsinki 00180, Finland

7 Department of Pathology, University of Helsinki and Helsinki University Hospital, Helsinki 00014, Finland

8 Turku Prostate Cancer Consortium, University of Turku, Turku, Finland

9 Orion Pharma, Espoo 02200, Finland

Published online: 28 April 2026

Introduction

PDE3A plays a multifaceted role in multiple cellular processes, including cAMP degradation, phosphorylation, dephosphorylation, and signaling. Its functions extend to the regulation of protein isoforms, protein biosynthesis, and the activity of other proteins such as *PKA*, *PKG* and *SERCA2*. The diverse roles of *PDE3A* underscore its importance in physiological and pathological conditions, making it a potential target for therapeutic interventions and several treatments have been identified that modulate *PDE3A* activity, including 8-chloro-cyclic adenosine monophosphate, anagrelide, cilostamide, cilostazol, estradiol, milrinone, thrombin and trequinsin, These treatments have been shown to affect various biological processes, including platelet function, oocyte competence, and cancer cell growth. Anagrelide, cilostazol, milrinone, and cilostamide have been shown to downregulate *PDE3A* enzyme activity, impacting maturation of megakaryocytes and platelet function and oocyte development [1–4]. Thrombin, on the other hand, upregulates *PDE3A* activity, leading to a reduction in intracellular cyclic AMP concentration in human platelets [5, 6]. Other treatments such as 8-chloro-cyclic adenosine monophosphate, trequinsin, and anagrelide also affect modulate *PDE3A* functionality, with implications for cancer cell growth and apoptosis [7–10]. In cancers, the PDE3A gene has been found to be highly expressed in e.g., melanoma [11, 12], glioblastoma [13], ovarian cancers [14], pancreatic ductal adenocarcinoma [15], and different molecular subtypes of sarcomas including gastrointestinal stromal tumor (GIST) [16] and myxoid liposarcoma [17]. This high *PDE3A* expression when accompanied with co-expression of *SLFN12* has been associated with the potential for *PDE3A-SLFN12* modulators to be used as a therapeutic strategy in these types of cancer [12–14, 17]. Recent studies have described in detail the molecular mechanism how molecular glue compounds called velcrins induce *PDE3A-SLFN12* complex formation and activate the specific RNase function of *SLFN12* towards $tRNA^{Leu}$(TAA) substrate digestion resulting in stalling of protein synthesis and apoptosis [13, 18–20]. However, further research is needed to fully understand the frequency and role of high *PDE3A-SLFN12* expression in different cancers, to assess whether on-target toxicities such as severe thrombocytopenia or cardiovascular side effects limit clinical use, and to develop effective biomarker guided therapeutic strategies for *PDE3A* modulation sensitive tumors.

To extend target validation of *PDE3A* across different human cancers, we used patient-derived functional ex vivo tumor models to study the correlation between *PDE3A* and *SLFN12* expression and therapeutic efficacy of *PDE3A* modulation in different cancers. Vital tumor cells isolated directly from surgical tissue sample, needle biopsy or malignant effusion of 250 individual patients, representing 24 major anatomical cancer types and 59 different histological or molecular subtypes were utilized for comparative reverse-phase-protein array (RPPA) -based protein expression analysis of *PDE3A* and *SLFN12* and parallel ex vivo drug screening of anagrelide. Results of the study validate high expression of the targets in subsets of brain tumors, melanomas and sarcomas and reveal potential novel indications for repurposing and further therapeutic development of *PDE3A* modulators including subsets of bladder-, cholangio-, endometrial-, and head and neck cancers. Individual anagrelide responsive tumors were also identified among breast, lung and pancreatic cancers. The performed analysis is to date the broadest reported pan-cancer ex vivo target evaluation study including both the highest number of individual patient samples and different cancer types included in any single reported ex vivo drug screening study.

Materials and methods

Patient samples

Patient samples were collected between 2016 and 2024 in context of four ongoing clinical studies focusing on the development of ex vivo drug screening techniques. The use of patient samples was approved by the Finnish National Supervisory Authority for Welfare and Health (V/39,706/2019), regional ethics committee of the University of Turku (51/1803/2017, 166/1801/2015), University of Turku Hospital (T295/2023, 64 /1801/2022, T0/021/18 and T180/2013-1), Auria biobank scientific board (AB19-6863 and AB18-2741), the regional ethics committee of the wellbeing services county of Southwest Finland (3/1801/2013) and the regional ethics committee of the Central Finland Healthcare District, Jyväskylä medical center (KSSHP/3U/2015). All experiments were undertaken with the understanding and written consent of the patients and the study methodologies conformed to the standards set by the Declaration of Helsinki. Altogether, 250 patient samples representing 24 major anatomical cancer types were included in the study. The patients were identified after confirming the biopsies taken from the tumor and the analyses performed by a pathologist. Thereafter, the selected patients were invited to participate and sign a written informed consent by the treating clinician at the study centers. The tissue samples were collected during routine operations performed as part of the patients´ standard care and only excess tissue left over from any diagnostic procedures were used for the study. Live unfixed tissues were placed into a sterile RPMI-1640 medium (Gibco) and delivered to the

research laboratory for immediate ex vivo drug screening. Upon receipt at the laboratory, a 1–5 mm^3 fragment of the bulk tumor tissue was collected and snap frozen for later preparation of a lysate sample for the reverse-phase-protein array analyses. A total of 1×10^4 to 1×10^5 isolated live cells were used for the ex vivo drug screening immediately on day of the operation. All cell culture experiments were performed in standard cell culture conditions (37 °C, 5% CO2) in RPMI–1640 medium supplemented with penicillin/streptomycin (100 units/100 mg), l-glutamine (2 mmol/L), 1x ITS-G (Gibco) and fetal bovine serum (1%, Biowest). GIST882 reference cell line was kindly provided by Dr. Jonathan Fletcher (Harvard Medical School, Boston, MA, USA).

Ex vivo drug screening

Ex vivo drug test with anagrelide (Selleck Biochemicals) was performed with four doses; 5000, 2500, 1250 and 625nM in 384-well microplate [20, 21]. Briefly, cells isolated from the tumor tissues by mechanical and enzymatic dissociation were dispensed as a single cell suspension into a 384-well plate readily containing the drugs and the controls (DMSO, staurosporin and imatinib). Cells were incubated with the drugs in standard cell culturing conditions (37 °C, 5% CO_2) for 96-hours and analyzed using an enzymatic cell viability assay CellTiter-Glo (Promega) according to the manufacturer´s instructions with a luminescence plate reader (Labrox, Turku, Finland) [22].

Reverse-phase protein array (RPPA) analysis

1–5 mm^3 of fresh bulk tumor tissue or 1×10^5 cells pelleted from malignant effusion samples were collected from all included patient samples and used to prepare a lysate sample for the RPPA array printing [23]. Pellet extracted from sarcoma cell line GIST882 was used as a reference sample. Samples were lysed in 20 µl of lysis buffer containing 100 mM Tris (pH 8.0), 0.2% SDS and 25 mM DTT. Prior to array printing, the lysates were denatured in 95 °C for 15 min. Denatured lysates were printed in random order with two replicates onto nitrocellulose-coated glass slides (Grace Biolabs, #305177) with a Genetix QArray Mini Arrayer (Molecular Devices). Primary antibodies used for reverse-phase protein array experiments were anti-PDE3A (#HPA014492, Sigma-Aldrich), anti-SLFN12 (ab234418, Abcam) and anti-PDE3B (#HPA024342, Sigma-Aldrich). Secondary detection was performed with a goat anti-mouse IgG conjugated to DyLight 680 (#35518, Thermo Pierce) and goat anti-rabbit IgG conjugated to DyLight 800 (#35571, Thermo Pierce) antibodies. For total protein measurement, the arrays were stained with a Sypro Ruby Blot solution (Invitrogen) and an antibody for actin (#4970, Cell Signaling Technology). The slides were scanned with a Tecan LS Reloaded (Tecan) microarray scanner to detect the Sypro signals for total protein and Odyssey Licor IR-scanner (LI-COR Biosciences) to detect the antibody signals. Array-Pro Analyzer microarray analysis software (V6.3, Media Cybernetics) was used for analyzing the data. Antibody signals were normalized to the Sypro total protein and z-score standardized. Z-scores < -2.0 or > 2.0 (−/+ 2×standard deviation from the whole sample collection) were considered as significantly down-regulated or up-regulated, respectively. Box plots and Pearson correlation analyses were created on GraphPad Prism (v.10.4.1) software. Results of the RPPA analysis are provided in Supplementary Table 1.

Statistical analysis

Ex vivo drug screening data were analyzed using normalized growth rate inhibition metric (GR score) yielding per-division metrics for drug potency and efficacy as described [24]. Briefly, dose response of the tumor samples to anagrelide was measured as % viability normalized to DMSO control treatment (negative control), 5 µM staurosporin (positive control), and 2 µM aphidicolin [24, see Eq. 1 in Statistical Analysis] and used for calculation of a GR score averaged across the full concentration range. GR score was calculated using R version 4.3.3, IC_{50} value calculations were performed with Prism statistical software (v.10.5.0), RPPA signal analyses were performed with Microsoft Excel. Statistical analyses of *PDE3A* and *SLFN12* expression levels and GR score-based response to anagrelide in different cancer types was done by performing a Kolmogorov-Smirnov (K-S) based enrichment analysis using the R-package stats (R Core Team 2024). Standardized mean protein expression or GR score values across all cell lines were ranked in descending order and the D-statistic (D), calculated as a running sum of the differences between the cumulative distributions of the cancer-specific subset and the full dataset to account for the skewedness of the distributions, was used as an enrichment score. Statistical significance was assessed using the K-S test, with exact p-values calculated via 10 000 Monte Carlo simulations. In silico analyses of the association between the PDE3A and SLFN12 mRNA expression (logTPM + 1) and anagrelide response (area under dose-response curve, AUC) were evaluated with cell line data from the Cancer Cell Line Encyclopedia (CCLE, $n = 476$) derived from DepMap using linear regression. The gene expression and AUC values were standardized to z-scores prior to analysis. Models included terms for PDE3A and SLFN12 and their interaction to assess both individual and joint associations with drug response. Statistical significance of model coefficients was evaluated using t-tests, and

model fit was summarized using the coefficient of determination (R^2) [25].

Results

Pan-cancer RPPA analysis of *PDE3A* and *SLFN12* protein expression

RPPA protein array technology was used to assess *PDE3A* and *SLFN12* protein level expression in patient-derived tumor samples. Altogether 250 patient samples representing 24 major anatomical cancer types and 59 different molecular or histological subtypes with 44% of samples derived from a primary tumor were included in the study (Fig. 1a). The RPPA analysis identified that the baseline expression level of *PDE3A* and *SLFN12* did not vary significantly between majority of the tumor samples but a subset of tumors representing different cancer types expressed high levels of both *PDE3A* and *SLFN12* (Fig. 1b-c), though still lower than in a high expressing positive control reference cell line GIST882 [16] (Fig. 1d). High expression of *PDE3A* (z-score ≥ + 2) was detected in 6.4% (n = 16) (Fig. 1b) and high expression of *SLFN12* (z-score ≥ + 2) in 7.7% (n = 19) of the analyzed samples (Fig. 1c). Tumors with the highest *PDE3A* and *SLFN12* expression levels included melanomas and sarcomas (Fig. 1d-e). Expression level distribution analysis highlighted statistically significant enrichment of *PDE3A* expression (K-S test D = 0.333, p = 5.40 × 10^{-3}) and *SLFN12* expression (K-S test D = 0.418, p = 4.00 × 10^{-4}) in sarcomas (Fig. 1c). Other individual tumor samples with high expression (z-score ≥ + 2) were derived from cholangiocarcinoma, head and neck-, renal-, lung- and ovarian cancers (Fig. 1d). Overall, *PDE3A* and *SLFN12* displayed a significant co-expression pattern (R^2 = 0.83) across all cancer types (Fig. 1e).

Pan-cancer ex vivo assessment of anagrelide therapy efficacy

Anagrelide was granted approval by the FDA in March 1997 for the treatment of essential thrombocythemia as a *PDE3A*

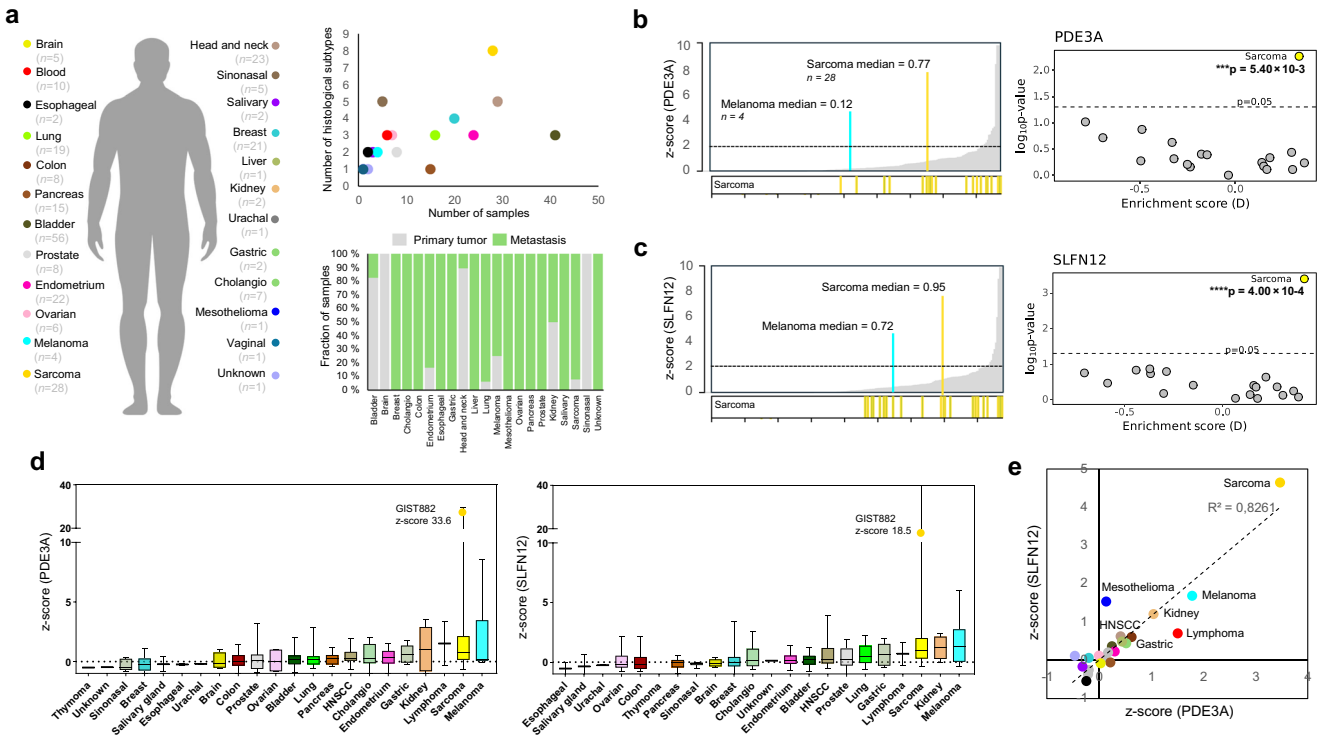

Fig. 1 Reverse phase protein array (RPPA) screen for PDE3A and SLFN12 expression in patient derived tumor samples. **(a)** 250 tumor cell samples collected from 24 major anatomical cancer types and representing 59 different histological or molecular subtypes were included in the study. 44% of the samples were derived from a primary tumor and 56% from a metastatic tumor. **(b)** Histogram showing the z-score distribution of the RPPA quantified PDE3A expression level across all samples (left) and scatter plot showing significant K-S based enrichment of PDE3A expression in the different anatomical cancer types (right). **(c)** Histogram showing the z-score distribution of the RPPA quantified SLFN12 expression level across all samples (left) and scatter plot showing significant K-S based enrichment of SLFN12 expression in the different anatomical cancer types (right). **(d)** Box plots showing the cancer type -level expression distribution of PDE3A (left) and SLFN12 (right) across all cancer types. Positive reference cell line sample GIST882 shown with a separate dot together with the sarcoma patient samples. **(e)** A scatter plot showing the correlation of the cancer type averaged expression levels of PDE3A and SLFN12

inhibitor [26]. Since then, several studies have shown that anagrelide displays also significant anti-cancer potential by inducing cancer cell growth inhibition and cell death by promoting complex formation of *PDE3A* and *SLFN12* [9, 27]. To evaluate therapeutic activity of anagrelide in different human cancers we compared its efficacy in the collected patient-derived tumor samples using ex vivo drug screening [21–23]. Vital tumor cells isolated immediately on the day of operation by enzymatic dissociation of the tumor tissues were used for high-throughput drug screens where anagrelide was included as one of the tested therapeutic drugs [21–23]. Tissue derived single cell milieu suspensions were exposed to anagrelide with a concentration range of 625 nM to 5 µM for 96 h after which cell viability was measured using an enzymatic cell viability assay [28]. To identify cancers most sensitive to anagrelide we compared the efficacy between the samples based on growth rate corrected (GR score) drug responses [24] and based on calculated IC_{50} estimates (Fig. 2a-b). Based on the growth rate normalized drug responses, 14/250 samples were found to be sensitive to anagrelide with a potent cytotoxic therapeutic response to the drug (GR score < 0), while an additional 79/250 samples showed sensitivity through growth inhibition (GR score 0–1) (Fig. 2a). The IC_{50} of anagrelide varied from 97 nM up (Fig. 2b). The most sensitive sample with anagrelide IC_{50} of 97 nM was a GIST tumor sample while the second most sensitive sample with IC_{50} of 130 nM was derived from recurrent BRAF V600E mutant skin melanoma (Fig. 2c). For comparison, the IC_{50} of anagrelide in the reference GIST model cell line GIST882 is 24nM [16]. Overall, the IC_{50} of anagrelide was < 1µM in 5 patient samples (2%), 1 to 5µM in 30 patient samples (12%) and 5 to 10µM in 23 patient samples (9.2%) (Fig. 2b). No dose dependent response to anagrelide was seen in 82/250 samples (32.8%). Based on comparison of the tumor type level efficacy, anagrelide was found to display highest median therapeutic activity in cholangiocarcinoma, sinonasal cancer, endometrial cancer, melanoma and sarcoma samples, the last two being the cancer types with the highest expression level of *PDE3A* and *SLFN12* on basis of the RPPA expression profiling (Figs. 1e and 2c). Across all evaluated cancer types, anagrelide displayed the most statistically significant therapeutic activity on basis of the GR score in sarcomas (K-S test D = -0.30, $p = 0.015$) and endometrial cancers (K-S test D = -0.30, $p = 0.021$) (Fig. 2d), with sarcoma derived samples also being the most responsive group also on based on IC_{50} distribution (Fig. 2e).

Anagrelide therapy efficacy and target expression in different sarcomas

Expression level of *PDE3A* and *SLFN12* was found to be highest in sarcomas in the pan-cancer RPPA analysis (Fig. 1e). Similarly, the *PDE3A-SLFN12* molecular glue anagrelide demonstrated best ex vivo therapy efficacy in the sarcoma tumor samples (Fig. 2d). The single most sensitive outlier response was seen in a GIST derived patient sample with

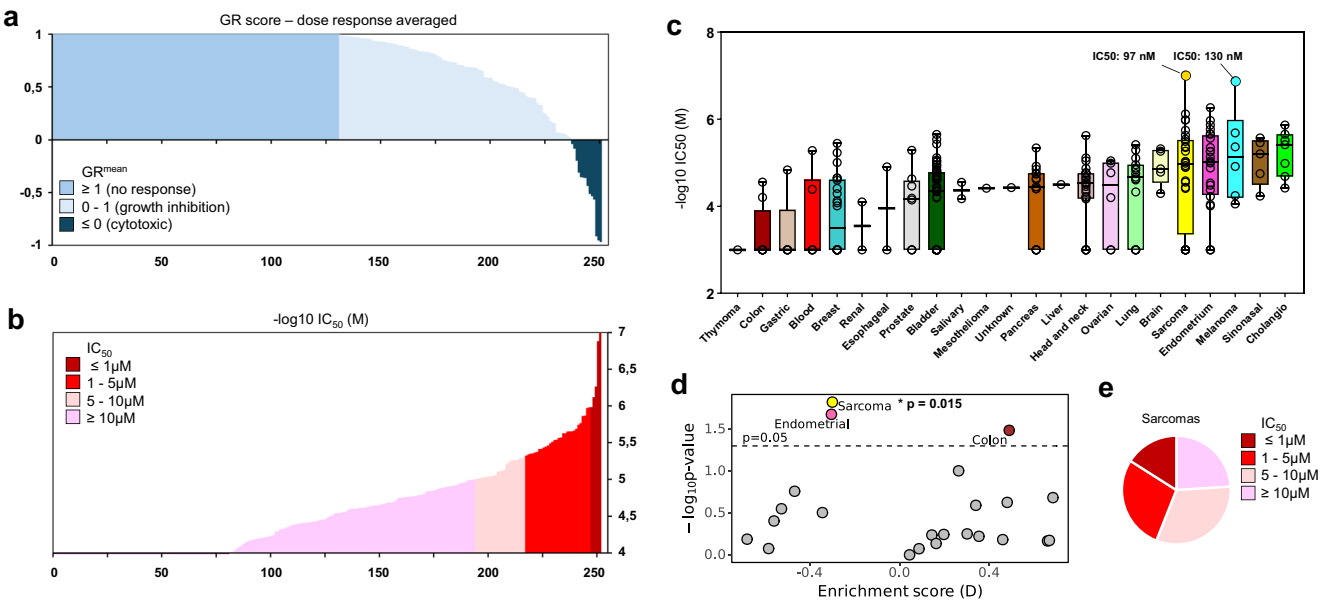

Fig. 2 Pan-cancer ex vivo analysis of anagrelide therapy efficacy. **(a)** Waterfall plot showing the dose response averaged GR score of anagrelide across all tested tumor samples. **(b)** Histogram showing the IC_{50} distribution (-log10 IC_{50} M) of anagrelide. **(c)** Box plot showing the IC_{50} distributions of anagrelide across all tested cancer types with the two most sensitive samples highlighted. **(d)** Scatter plot showing K-S based enrichment of anagrelide GR score in all tested cancer types. Endometrial cancer and sarcoma were identified as the most sensitive cancer types. **(e)** Pie chart showing the percentage of sarcoma samples stratified according to IC_{50} defined anagrelide sensitivity

an IC_{50} of 97 nM. To gain more insights into expression of *PDE3A* and *SLFN12* in the specific sarcoma types, and to the correlation with response to anagrelide, a detailed comparison was conducted dividing the samples according to pathological diagnosis into seven groups; (1) fibrosarcoma, (2) GIST, (3) leiomyosarcoma, (4) liposarcoma, (5) osteosarcoma, (6) other types including alveolar soft tissue sarcoma, desmoplastic small round cell tumor (DSRCT), chondrosarcoma hemangiopericytoma, malignant peripheral nerve sheath tumor (MPNST) and, (7) samples with missing info on histological subtype (unknown). As the PDE3 family includes two proteins, *PDE3A* and *PDE3B*, which show structural similarity [29], we performed a repeat RPPA analysis of the sample cohort also for expression of *PDE3B* to assess if anagrelide therapy efficacy correlates similarly with the expression level of *PDE3B* (Fig. 3a-b). Across the main anatomical cancer types, *PDE3B* was not found to be expressed at a significantly higher level in any individual cancer type compared to other tumor types. On average, the highest average expression levels were seen in brain tumor, hematological and liver cancer samples (Fig. 3a) aligning with evidence from e.g., the Human Protein Atlas [30] and The Cancer Genome Atlas [31] on pan-cancer expression level of PDE3B. Individual tumor samples with high *PDE3B* levels were identified also among renal, ovarian, head and neck, lung, melanoma and breast cancer samples (Fig. 3a). No statistically meaningful pan-cancer correlation between the expression levels of *PDE3B* with either *PDE3A* or *SLFN12* was observed (Fig. 3b). Samples of hematological origin displayed the highest relative expressions of all three proteins (Fig. 3b).

For sarcoma subtype separated analysis, we compared the expression levels of *PDE3A*, *PDE3B* and *SLFN12* across the sarcoma samples (Fig. 4a). *PDE3A* was found to be expressed at the highest level in an alveolar soft tissue sarcoma sample (Supplementary figure S2), followed by two fibrosarcoma samples. *SLFN12* was similarly expressed at high level in the same alveolar soft tissue sarcoma sample and the two fibrosarcoma samples. High *SLFN12* expression was also observed in the GIST tumor sample displaying exceptional sensitivity to anagrelide (IC_{50} 97 nM) (Fig. 4b). Overall, anagrelide therapy efficacy was found to have a slightly stronger positive correlation with the expression level of *SLFN12*, though an individual fibrosarcoma sample (sample #53) with high expression of both *PDE3A* and *SLFN12* was found to be nonresponsive to anagrelide (no IC_{50}, GR_{mean} 1.03) (Fig. 4b). Median IC_{50} of anagrelide in the samples with *PDE3A* z-score≥2 was 4.45μM vs. 2.75μM in the samples with *SLFN12* z-score≥2 (p=0.011). *PDE3B* expression was highest in the GIST tumor samples as a group but no statistically significant correlation was observed between the expression level of *PDE3B* and the efficacy of anagrelide among the GIST or all sarcoma samples (Fig. 4b).

In silico validation of PDE3A-SLFN12 association with anagrelide response

To assess whether the observed relationship between PDE3A and SLFN12 expression and anagrelide responsiveness was consistent with publicly available datasets, the RNA expression of the genes in CCLE cell lines (n = 476) were compared against the cell lines´ responses to anagrelide on data derived from the DepMap dataportal [25]. Across all cell lines, a linear regression model including SLFN12 and PDE3A individually as well as an interaction term combining the two revealed significant associations with anagrelide therapeutic activity (dose response as AUC) (PDE3A $p < 2 \times 10^{-16}$, SLFN12 $p = 8.44 \times 10^{-7}$, PDE3A x SLFN12 $p = 1.79 \times 10^{-6}$) with higher expression of these genes associated with lower anagrelide AUC, consistent with increased drug sensitivity (Fig. 4c). Together these variables explained 24.83% of the variance in anagrelide AUC across these cell lines (R^2 = 0.2483). Limiting the analysis to only sarcoma cell lines (n = 21) yielded a similar pattern, where PDE3A expression and the PDE3A-SLFN12 interaction were found to be significantly associated with anagrelide response (PDE3A p = 0.0077, PDE3A x SLFN12

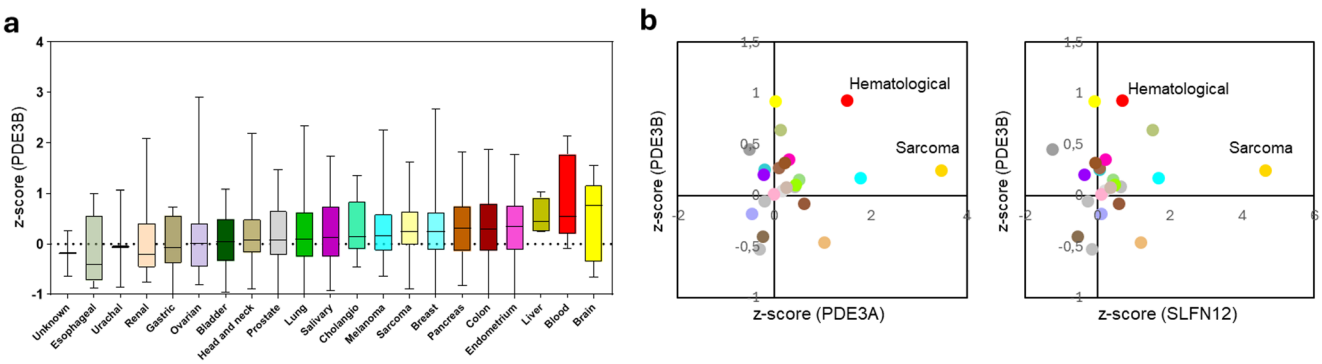

Fig. 3 RPPA analysis of PDE3B expression in patient derived tumor samples. **(a)** Box plot showing the cancer type -level expression distribution of PDE3B. **(b)** Scatter plots showing the correlation of the cancer type averaged expression levels of PDE3B with PDE3A (left) and PDE3B with SLFN12 (right)

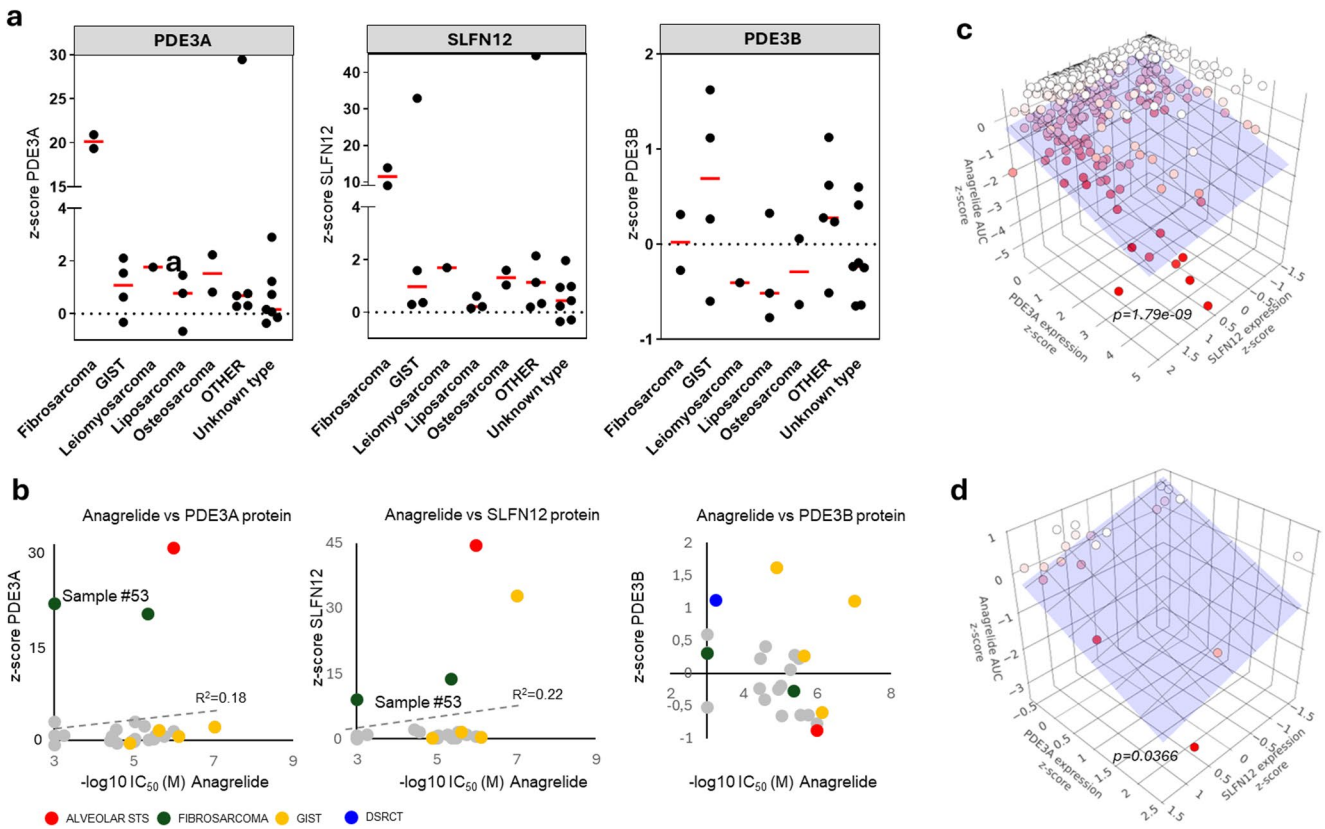

Fig. 4 Pan-sarcoma assessment of anagrelide therapy efficacy and correlation with target expression **(a)** Scatter plots showing the z-score for PDE3A, SFLN12 and PDE3B expression across the 25 included sarcoma samples divided to the different sarcoma types. **(b)** Scatter plots showing the correlation between PDE3A, SLFN12 and PDE3B expression (z-score) and anagrelide efficacy (IC_{50}). A fibrosarcoma sample (#245) with high expression of PDE3A and SLFN12 was non-responsive (no measurable IC_{50}). (**c**) 3D scatter plot showing the pan-cancer z-scores for PDE3A, SFLN12 and anagrelide AUC across 476 cell lines with data available through the DepMap data portal (https://depmap.org/portal/). (**d**) 3D scatter plot showing the pan-cancer z-scores for PDE3A, SFLN12 and anagrelide AUC across 21 sarcoma cell lines with data available through the DepMap portal

$p = 0.0366$), explaining 45.6% of the variance in anagrelide AUC ($R^2 = 0.456$), again indicating that higher expression corresponded with lower anagrelide AUC and increased drug sensitivity (Fig. 4d).

Discussion

Ex vivo drug screening is currently in the focus of intense research and development efforts globally as a strategy to assist precision cancer medicine and assessment of therapy efficacy for individual patients. In addition to this core purpose, ex vivo drug screening is also well suited to support target discovery and drug development efforts in context of cancer drug development. In this study we took advantage of our ongoing ex vivo drug screening activities and the collected patient derived functional tumor samples to evaluate the therapeutic potential of *PDE3A-SLFN12* modulation of approved drug anagrelide across various cancer types. Several solid tumors, such as melanoma, sarcoma, glioblastoma, and ovarian cancer have been previously shown to co-express the proteins *PDE3A* and *SLFN12*. Therapeutic molecular glues called "velcrins" can be used to induce complex formation of *PDE3A* and *SLFN12* which leads to a cytotoxic response in cells by stimulating the RNase activity of *SLFN12*. Here, we included 250 patients representing 24 different major anatomical cancer types into an RPPA-based protein expression level profiling of *PDE3A*, *SLFN12* and *PDE3B* and for functional ex vivo analysis of sensitivity of the samples to anagrelide treatment. Protein expression analysis was performed directly from tumor lysates using RPPA technology and drug sensitivity was assessed using high-throughput ex vivo drug screening [21–23]. Comparative analyses of target expression and drug sensitivity were used to gain insights in the sensitivity of different cancers to *PDE3A-SLFN12* complex formation induced by anagrelide and to identify potential tumor and cancer type specific patterns of sensitivity and target expression. Results of the study highlight high expression of *PDE3A* and *SLFN12* especially across different histological subtypes of sarcoma and melanoma, which were also the cancer types most sensitive to anagrelide

treatment. High expression of *PDE3A* and *SLFN12* was also observed in select patient samples derived from cholangiocarcinoma, head and neck, lung and ovarian cancers. Across all tested cancer types, the therapeutic efficacy of anagrelide was found to closely follow the expression profiles of both *PDE3A* and *SLFN12* and a comparable, albeit more modest trend could also be observed in established cancer cell lines based on public data from the DepMap [25]. In sarcoma samples, anagrelide was found to display exceptional therapeutic efficacy in a *PDE3A-SLFN12* positive GIST, an alveolar soft tissue sarcoma and a fibrosarcoma case, consistent with findings from previous studies [16, 32]. In conclusion, the observations support previous findings that *PDE3A-SLFN12* modulation could serve as a novel and effective therapeutic mechanism of action in melanomas, GIST and select other sarcoma subtypes expressing *PDE3A-SLFN12* [12, 16, 33]. However, it should be considered that the different subtypes of sarcomas compose a highly heterogeneous group of cancers, and the expression level of the target genes can vary significantly between and within different sarcoma subtypes as evident from sarcoma model cell lines and sarcoma patient samples [34] (Supplementary figure S3). Thus, for biomarker purposes, to predict sensitivity to *PDE3A-SLFN12* modulation, the absolute expression levels of the targets might not be sufficient on their own. This is particularly apparent in the endometrial cancer cohort, which exhibited sensitivity to anagrelide treatment despite lacking significant elevation in *PDE3A* or *SLFN12* expression as a group. Additionally, in the sarcoma cohort, two fibrosarcoma samples displayed high expression of both *PDE3A* and *SLFN12* (Fig. 4b), but a therapeutic response to anagrelide was observed only in one of the two. Here, the result could reflect biological differences related to cell of origin [34] or cellular differentiation as suggested by the slightly different histopathological classifications of the samples. The anagrelide responsive sample (#47) was originally classified as a fibrosarcoma/myxofibrotic sarcoma while the non-responsive sample (#53) was originally classified as a fibrosarcoma/liposarcoma. Thus, the discrepancy in anagrelide sensitivity between these two samples could result from molecular characteristics independent of the target expression levels. Moreover, considering the recent results reported from clinical development of a novel *PDE3A-SLFN12* molecular glue BAY 2,666,605 [12], it has become important to investigate effective dosing regimens, therapeutic windows, and innovative administration strategies [35] to determine how to safely harness the anticancer potential of *PDE3A-SLFN12* modulation and to avoid the potential severe on-target off-tumor toxicities related to expression of *PDE3A-SLFN12* in benign cell types.

Limitations of the study

While our study underscores the translational potential of *PDE3A-SLFN12* modulation across different cancer types and individual patient tumors, it does not comprehensively investigate the precise molecular and genetic background in which the *PDE3A-SLFN12* complex formation results in potent cytotoxic response. The patient derived tumor samples utilized in this study were collected for the purpose of establishing methods for ex vivo drug screening with limited molecular profiling data available thus limiting the possibility of performing multiomics data integration including correlation with genetic alteration or detailed histogical/pathological information. Although a statistically significant correlation between *PDE3A-SLFN12* protein expression and the therapeutic efficacy of anagrelide was observed, individual samples including different sarcomas were found non-responsive despite high *PDE3A-SLFN12* expression levels. This discrepancy could reflect biological differences between the samples but can also be derived from technical limitations of ex vivo drug screening. While a bulk tissue used for assessment of target expression in the sample may be representative of the tumor, the vital cell sample derived from the same tissue may not always be successful and thus representative of the tumor. Viability and number of successfully isolated cells can vary from tissue to tissue and affect accuracy of the drug screening results. Especially certain sarcoma tumor tissues can be challenging for isolation of vital cells for ex vivo culture due to low cellular density and/or high density of the ECM composing the bulk of the tumor mass. In summary, sarcomas are heterogenous group of tumors and further studies in patient-derived sarcoma samples with parallel histopathological and molecular profiling could provide more comprehensive insights into the applicability and efficacy of therapeutic targeting of *PDE3A-SLFN12* in different sarcoma subtypes.

Supplementary Information The online version contains supplementary material available at https://doi.org/10.1007/s00109-026-02677-7.

Authors' contributions Conceptualization: JKR and HS; methodology: JKR, NL, KR, and EV; investigation: NL, KR, EV, JS and JKR; visualization: JKR and JS; funding acquisition: JKR; project administration: JKR, JK, SV and PT; supervision: JKR; writing – original draft: JKR, KR, NL, JS and HS; writing – review and editing: JKR, HS, JS, KR and NL.

Funding The authors declare that no funds, grants, or other support were received during the preparation of this manuscript.

Data availability The dataset generated and analyzed in the current study is provided as supplemental online material.

Declarations

Ethics approval and consent to participate Patient samples were collected between 2016 and 2024 in context of four ongoing clinical studies. The use of patient samples was approved by the Finnish National Supervisory Authority for Welfare and Health (V/39,706/2019), regional ethics committee of the University of Turku (51/1803/2017, 166/1801/2015), University of Turku Hospital (T295/2023, 64 /1801/2022, T0/021/18 and T180/2013-1), Auria biobank scientific board (AB19-6863 and AB18-2741), the regional ethics committee of the wellbeing services county of Southwest Finland (3/1801/2013) and the regional ethics committee of the Central Finland Healthcare District, Jyväskylä medical center (KSSHP/3U/2015). All experiments were undertaken with the understanding and written consent of the patients and the study methodologies conformed to the standards set by the Declaration of Helsinki. Clinical trial number: not applicable.

Competing interests Harri Sihto is a shareholder in Sartar Therapeutics Oy. Juha K. Rantala is the founder of Misvik Biology Oy and an employee of Orion Pharma. Kiesha Rice, Janne Suhonen, and Eetu Välimäki are employees of Misvik Biology Oy. Noora Lehtinen and Juha Kononen are employees of Docrates Mehiläinen Oy. The other authors have declared no competing interests.

References

1. Coenen DM, Heinzmann ACA, Oggero S, Albers HJ, Nagy M, Hagué P, Kuijpers MJE, Vanderwinden JM, van der Meer AD, Perretti M, Koenen RR, Cosemans JMEM (2021) Inhibition of phosphodiesterase 3A by cilostazol dampens proinflammatory platelet functions. Cells 10(8):1998
2. Taiyeb AM, Alazzam A, Kjelland ME, Adams TH, Kraemer DC, Muhsen-Alanssari SA, Ridha-Albarzanchi MT (2020) A rapid and efficient method for the collection of highly developmental murine immature oocytes using cilostazol, a phosphodiesterase 3A inhibitor. Life Sci 241:117100
3. Roy PK, Qamar AY, Tanga BM, Fang X, Kim G, Bang S, Cho J (2021) Enhancing oocyte competence with milrinone as a phosphodiesterase 3A inhibitor to improve the development of porcine cloned embryos. Front Cell Dev Biol 9:647616
4. Gupta A, Trigun SK (2022) Cilostamide, a phosphodiesterase 3A inhibitor, sustains meiotic arrest of rat oocytes by modulating cyclic adenosine monophosphate level and the key regulators of maturation promoting factor. J Cell Biochem 123(12):2030–2043
5. Zhang W, Colman RW (2007) Thrombin regulates intracellular cyclic AMP concentration in human platelets through phosphorylation/activation of phosphodiesterase 3A. Blood 110(5):1475–1482. https://doi.org/10.1182/blood-2006-10-052522
6. Hunter RW, Mackintosh C, Hers I (2009) Protein kinase C-mediated phosphorylation and activation of PDE3A regulate cAMP levels in human platelets. J Biol Chem 284(18):12339–12348. https://doi.org/10.1074/jbc.M807536200
7. Garvie CW, Wu X, Papanastasiou M, Lee S, Fuller J, Schnitzler GR, Horner SW, Baker A, Zhang T, Mullahoo JP, Westlake L, Hoyt SH, Toetzl M, Ranaghan MJ, de Waal L, McGaunn J, Kaplan B, Piccioni F, Yang X, Lange M, Tersteegen A, Raymond D, Lewis TA, Carr SA, Cherniack AD, Lemke CT, Meyerson M, Greulich H (2021) Structure of PDE3A-SLFN12 complex reveals requirements for activation of SLFN12 RNase. Nat Commun 12(1):4375
8. Ai Y, He H, Chen P, Yan B, Zhang W, Ding Z, Li D, Chen J, Ma Y, Cao Y, Zhu J, Li J, Ou J, Du S, Wang X, Ma J, Gao S, Qi X (2020) An alkaloid initiates phosphodiesterase 3A-schlafen 12 dependent apoptosis without affecting the phosphodiesterase activity. Nat Commun 11(1):3236
9. An R, Liu J, He J, Wang F, Zhang Q, Yu Q (2019) PDE3A inhibitor anagrelide activates death signaling pathway genes and synergizes with cell death-inducing cytokines to selectively inhibit cancer cell growth. Am J Cancer Res 9(9):1905–1921
10. Chen J, Liu N, Huang Y, Wang Y, Sun Y, Wu Q, Li D, Gao S, Wang HW, Huang N, Qi X, Wang X (2021) Structure of PDE3A-SLFN12 complex and structure-based design for a potent apoptosis inducer of tumor cells. Nat Commun 12(1):6204. https://doi.org/10.1038/s41467-021-26546-8
11. Zhong F, Liu J, Gao C, Chen T, Li B (2022) Downstream regulatory network of MYBL2 mediating its oncogenic role in melanoma. Front Oncol 12:816070
12. Papadopoulos KP, McKean M, Goldoni S, Genvresse I, Garrido MF, Li R, Wilkinson G, Kneip C, Yap TA (2024) First-in-human dose-escalation study of the first-in-class PDE3A-SLFN12 complex inducer BAY 2666605 in patients with advanced solid tumors coexpressing SLFN12 and PDE3A. Clin Cancer Res 30(24):5568–5576
13. Aquilanti E, Goldoni S, Baker A, Kotynkova K, Andersen S, Bozinov V, Gao GF, Cherniack AD, Lange M, Lesche R, Kopitz C, Lienau P, Lewis TA, Garrido M, Gradl S, Seidel H, Tseng YY, Ligon KL, Wen PY, Meyerson M, Greulich H (2024) Velcrin molecular glues induce apoptosis in glioblastomas with high *PDE3A* and *SLFN12* expression. Neurooncol Adv 6(1):vdae115. https://doi.org/10.1093/noajnl/vdae115
14. Nazir M, Senkowski W, Nyberg F, Blom K, Edqvist PH, Jarvius M, Andersson C, Gustafsson MG, Nygren P, Larsson R, Fryknäs M (2017) Targeting tumor cells based on Phosphodiesterase 3A expression. Exp Cell Res 361(2):308–315
15. Kumazoe M, Takai M, Hiroi S, Takeuchi C, Yamanouchi M, Nojiri T, Onda H, Bae J, Huang Y, Takamatsu K, Yamashita S, Yamada S, Kangawa K, Takahashi T, Tanaka H, Tachibana H (2017) PDE3 inhibitor and EGCG combination treatment suppress cancer stem cell properties in pancreatic ductal adenocarcinoma. Sci Rep 7(1):1917
16. Pulkka OP, Gebreyohannes YK, Wozniak A, Mpindi JP, Tynninen O, Icay K, Cervera A, Keskitalo S, Murumägi A, Kulesskiy E, Laaksonen M, Wennerberg K, Varjosalo M, Laakkonen P, Lehtonen R, Hautaniemi S, Kallioniemi O, Schöffski P, Sihto H, Joensuu H (2019) Anagrelide for gastrointestinal stromal tumor. Clin Cancer Res 25(5):1676–1687
17. Toivanen K, Kilpinen S, Ojala K, Merikoski N, Salmikangas S, Sampo M, Böhling T, Sihto H (2023) *PDE3A* Is a highly expressed therapy target in myxoid liposarcoma. Cancers (Basel) 15(22):5308
18. de Waal L, Lewis TA, Rees MG, Tsherniak A, Wu X, Choi PS, Gechijian L, Hartigan C, Faloon PW, Hickey MJ, Tolliday

N, Carr SA, Clemons PA, Munoz B, Wagner BK, Shamji AF, Koehler AN, Schenone M, Burgin AB, Schreiber SL, Greulich H, Meyerson M (2016) Identification of cancer-cytotoxic modulators of PDE3A by predictive chemogenomics. Nat Chem Biol 12(2):102–108
19. Lee S, Hoyt S, Wu X, Garvie C, McGaunn J, Shekhar M, Tötzl M, Rees MG, Cherniack AD, Meyerson M, Greulich H (2023) Velcrin-induced selective cleavage of $tRNA^{Leu}$(TAA) by SLFN12 causes cancer cell death. Nat Chem Biol 19(3):301–310
20. Lewis TA, Ellermann M, Kopitz C, Lange M, de Waal L, Wu X, Tersteegen A, Denner K, Lienau P, Kaulfuss S, Goldoni S, Meyerson M, Greulich H, Gradl SN (2024) Discovery of BAY 2666605, a Molecular Glue for PDE3A and SLFN12. ACS Med Chem Lett 15(10):1662–1667
21. Mäkelä R, Arjonen A, Suryo Rahmanto A, Härmä V, Lehtiö J, Kuopio T, Helleday T, Sangfelt O, Kononen J, Rantala JK (2020) Ex vivo assessment of targeted therapies in a rare metastatic epithelial-myoepithelial carcinoma. Neoplasia 22(9):390–398
22. Arjonen A, Mäkelä R, Härmä V, Rintanen N, Kuopio T, Kononen J, Rantala JK (2020) Image-based ex vivo drug screen to assess targeted therapies in recurrent thymoma. Lung Cancer 145:27–32
23. Nykänen N, Mäkelä R, Arjonen A, Härmä V, Lewandowski L, Snowden E, Blaesius R, Jantunen I, Kuopio T, Kononen J, Rantala JK (2021) *Ex Vivo* Drug screening informed targeted therapy for metastatic parotid squamous cell carcinoma. Front Oncol 11:735820
24. Hafner M, Heiser LM, Williams EH, Niepel M, Wang NJ, Korkola JE, Gray JW, Sorger PK (2017) Quantification of sensitivity and resistance of breast cancer cell lines to anti-cancer drugs using GR metrics. Sci Data 4:170166
25. Arafeh R, Shibue T, Dempster JM et al (2025) The present and future of the cancer dependency map. Nat Rev Cancer 25:59–73
26. Tefferi A, Silverstein MN, Petitt RM, Mesa RA, Solberg LA Jr (1997) Anagrelide as a new platelet-lowering agent in essential thrombocythemia: mechanism of actin, efficacy, toxicity, current indications. Semin Thromb Hemost 23(4):379–383
27. Meanwell NA, Anagrelide (2023) A clinically effective cAMP phosphodiesterase 3A inhibitor with molecular glue properties. ACS Med Chem Lett 14(4):350–361
28. Lehtinen N, Suhonen J, Rice K, Välimäki E, Toriseva M, Routila J, Halme P, Rahi M, Irjala H, Leivo I, Kallajoki M, Nees M, Kuopio T, Ventelä S, Rantala JK (2024) Assessment of targeted therapy opportunities in sinonasal cancers using patient-derived functional tumor models. Transl Oncol 44:101935
29. Degerman E, Belfrage P, Manganiello VC (1997) Structure, localization, and regulation of cGMP-inhibited phosphodiesterase (PDE3). J Biol Chem 272(11):6823–6826
30. Takanen JO, Hober S, Alm T et al (2015) Proteomics. Tissue-based map of the human proteome. Science 347(6220):1260419
31. Bartha Á, Győrffy B (2021) TNMplot.com: a web tool for the comparison of gene expression in normal, tumor and metastatic tissues. Int J Mol Sci 22(5):2622
32. Brodin BA, Wennerberg K, Lidbrink E, Brosjö O, Potdar S, Wilson JN, Ma L, Moens LN, Hesla A, Porovic E, Bernhardsson E, Papakonstantinou A, Bauer H, Tsagkozis P, von Sivers K, Wejde J, Östling P, Kallioniemi O, Stragliotto CL (2019) Drug sensitivity testing on patient-derived sarcoma cells predicts patient response to treatment and identifies c-Sarc inhibitors as active drugs for translocation sarcomas. Br J Cancer 120(4):435–443
33. Takaki EO, Kiyono K, Obuchi Y, Yamauchi T, Watanabe T, Matsumoto H, Karimine M, Kuniyoshi Y, Nishikori S, Yokoyama F, Nishimori H, Nabeshima H, Nakamura K (2024) A PDE3A-SLFN12 Molecular glue exhibits significant antitumor activity in TKI-resistant gastrointestinal stromal tumors. Clin Cancer Res 30(16):3603–3621
34. Hoadley KA, Yau C, Hinoue T, Cancer Genome JM, Benz CC, Laird PW et al (2018) Cell-of-origin patterns dominate the molecular classification of 10,000 tumors from 33 types of cancer. Cell 173(2):291–304.e6
35. Toivanen K, De Sutter L, Wozniak A, Wyns K, Merikoski N, Salmikangas S, Duan J, Maksimow M, Lahtinen M, Böhling T, Schöffski P, Sihto H (2025) Pharmacokinetic profile and *in vivo* anticancer efficacy of anagrelide administered subcutaneously in rodents. Drug Deliv 32(1):2463433